sensors

MDPI

Article

Monitoring a 28.5m high anchored pile wall in gravel using different sensors

Ricardo Moffat [1*], Pablo Parra[1] and Miguel Carrasco[1]

[1]Faculty of Engineering and Sciences, Universidad Adolfo Ibáñez, Santiago, Chile
* Correspondence: ricardo.moffat@uai.cl; Tel.: +56 22 331 1786 (R.M.)

Received: date; Accepted: date; Published: date

Abstract: Monitoring horizontal displacements of a pile wall with anchors on a 28.5m deep excavation using the top-down construction method has been performed using optical fiber (BOTDR), strain gauges, inclinometers and topographic survey. In this work we present a comparison between these different techniques to measure horizontal displacements in the pile at several stages of the soil excavation process. It was observed that displacements can be separated in two components: rigid body motion and pile flexural deformation. Measurements using optical fiber and inclinometers are considered the most adequate and easy to install. A numerical model allows to evaluate the influence of earth pressure on the estimated horizontal displacements. It is shown that using recommended loads on the wall represents correctly displacements observed on the field.

Keywords: Deep excavation; anchored wall; monitoring; pile displacement.

1. Introduction

Monitoring of soil slopes [1] and retaining walls [2] have shown useful to identify main factors that contribute to a safety design. Urban building excavations require stable support systems that can provide lateral support reducing the lateral deformation of these walls or piles to avoid or decrease its impact on surrounding structures as the walls or piles get larger, they require additional support systems such as anchors. In fact, every day is more common to use pre-stressed ground anchors using either tie rods or cable strands. As these elements are pre-stressed at the same time that the excavation is advancing, most of the displacement during construction could be prevented.

The geotechnical design frequently uses the limit state approach to check the adequacy of the structure against failure or a serviceability limit state. Then the structure is designed to satisfy a required factor of safety and deformations that are below serviceability limits depending of the type of structure. The adequate assess of the safety factor, and expected deformations, need to have an adequate characterization of the soil properties (strength parameters and deformation modulus) and reasonable theoretical or numerical methods to predict the loads over the retaining system.

The design of a multi-level anchored wall depends on factors such as [3]: Soil resistance and deformation modulus; flexibility of the wall; necessary displacements to develop earth pressure; applied anchor loads. The stress distribution behind a wall depends on the construction method or stages, anchor pre-stressing, and relaxation. Assuming that a fully active condition can be reached in this type of wall is not always accurate, as pre-stressed anchors do not allow free deformation and displacement of the soil as required to reach the active conditions. It is expected higher lateral stresses in zones closer to the anchor location as the anchors produce a condition that is closer to a passive state of the soil.

Different studies on deep excavation have been performed using numerical modeling or through monitoring displacements or strains of the walls. A 14.7m deep excavation was modeled by Hou et al. [4] using 3D finite-element analyses finding that soil anisotropy has a significant effect on wall deformation. Lam et al. [5] performed a series of centrifuge models of deep excavation in soft soils. They found that the trend lines given by Clough et al. [6] match their results and that small strain stiffness is very important in the deformation mechanism.

This research is based on a deep excavation 28.5m deep and extending 65m on the West-East and 95m on the North-South directions that was monitored in Santiago, Chile (located between 33° and 34°S at approximately 100 km from the coast line). Santiago´s basin is composed mainly of alluvial and fluvial sediments originated in the Maipo and Mapocho river basins. In most places the gravel deposit has a thickness over 100m. Santiago gravel is composed of boulders usually less than 20 cm in diameter in a matrix of soil that includes silty gravel to silty sand and some clayey lenses. Undisturbed soil samples have been tested in this material with samples of 1m diameter as shown in detail in [7]. Friction angles for these gravels have been found above 50°. Deformation modulus has been measured using large triaxial test on undisturbed soil samples and also using loading plate tests.

Results show an increase of deformation modulus of the soil, between 50 MPa at the surface, to 300 MPa at about 40m deep [8]. The pile wall consisted in 1m diameter pre-bored piles made of cast in place reinforced concrete with 2m center to center spacing. Each pile had three pre-stresses anchors, each anchor consisted in six steel cables (ASTM A416 GR270). This non-continuous pile wall was monitored using different measurement techniques to compare its performance on site. Numerical modeling was performed in order to carry out a parametric study of the influence of the main variables that affects wall displacements in practice. Interaction diagrams were also studied to check strength requirements of piles of different diameter.

2. Materials and Methods

Different sensors or instruments were used on the field to measure the displacements and strains of the non-continuous anchored wall (or piles). The following sections present the main characteristics of these instruments.

2.1. Inclinometer

The inclinometer is a 71 cm long probe with two accelerometers in its interior that allow to estimate the inclination in two perpendicular directions with respect to the vertical position. The necessary casing was installed on the field during the pile construction as shown in Figures 1. Measurements were taken every 0.5m. Data was transmitted to the surface by Bluetooth and saved by the data acquisition system (iPAQ hx2410) located on the surface. Table A1 shows the main characteristics of the casing, and Table A2 shows the main characteristics of the inclinometer. An initial or base measurement was carried out when the pile was constructed, but before the excavation started.

2.2 Strain gauges

Strain gauges model PFL-20-15 (gage factor of 2.12 + 1% and thermal expansion coefficient of 118 × 10^{-6} /°C) were used to measure the internal pile deformations. Figure 2 shows the strain gauge attached to one side of the steel reinforcing bar, polished prior installation.

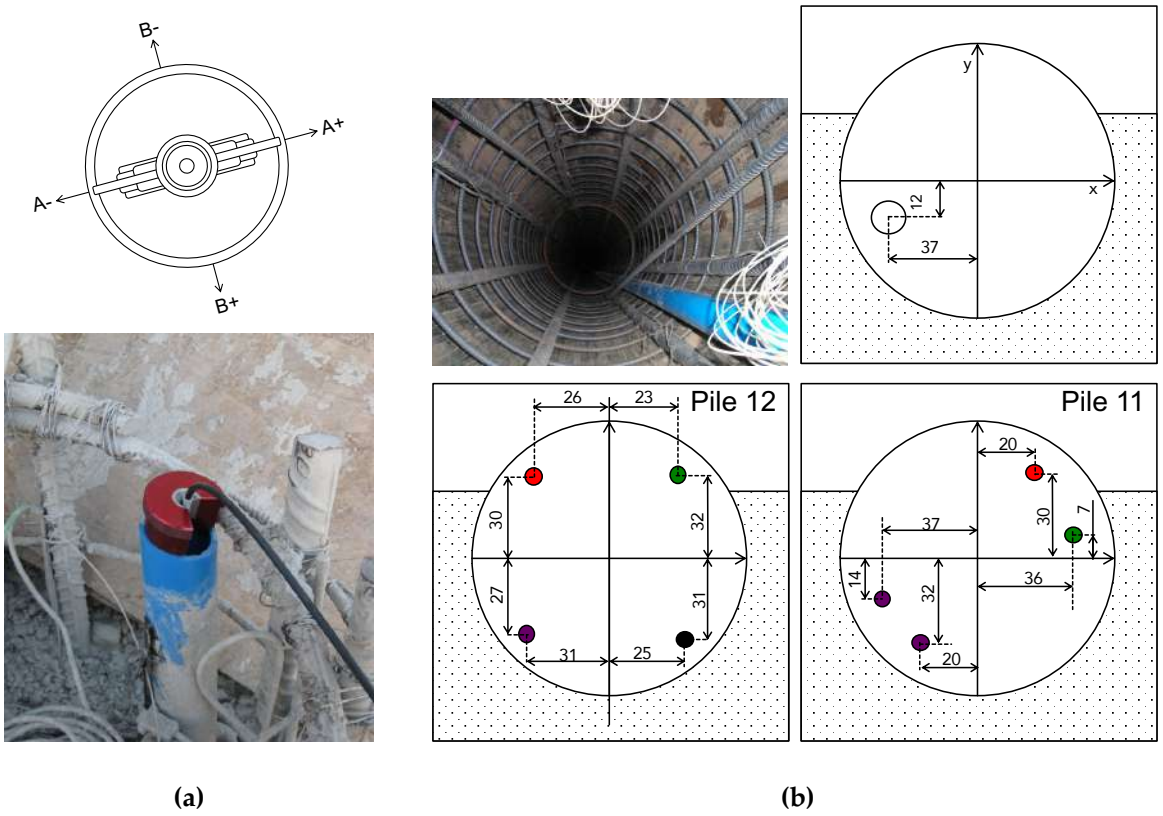

(a) **(b)**

Figure 1. (**a**) Inclinometer inside casing installed in pile; (**b**) Installation and location of the inclinometer casing.

These sensors were installed in the piles to measure longitudinal and shear strains. Two piles (piles 11 and 12) were instrumented with strain gauges. In pile 11 these were located every 2 m along the pile length, and every 4 m for the case of pile 12. Figure 1b shows a schematic cross section.

The relation between length and resistance in the strain gauge is given by:

$$GF = \frac{\Delta R}{R} / \frac{\Delta L}{L} \quad (1)$$

where: *GF*: gain factor; *R*: original resistance of the strain gauge (120 ohms); *L*: original strain gauge length. An acquisition system SCXI-of 16 bits of resolution and maximum sampling rate of 200 Ks/S was used to obtain the data.

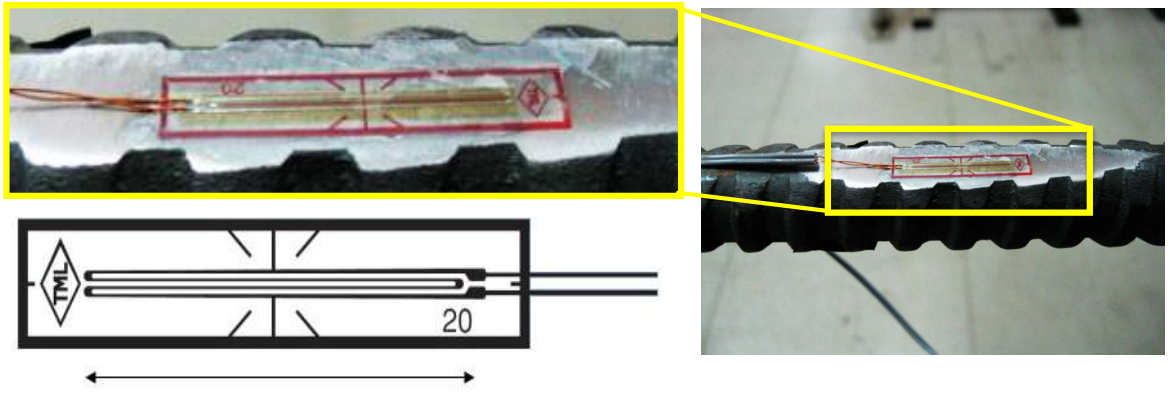

Figure 2. Photo of installed strain gauges ion reinforcement of piles (Photo of strain gauge PFL-20-11)

92 *2.2 Optical fiber*

93 A Brillouin spectroscopy and Optical Domain Reflectometry (BOTDR), as shown in Figure 3a,
94 enables to measure the longitudinal strain on optical fibers. Deformation in the longitudinal direction of
95 the fiber generates a frequency shift that is proportional to the fiber strain (see Figure 3b). The BOTDR
96 equipment is able to measure the shift in Brillouin frequency and the time interval between launching
97 pulse light and the received scattered light. Therefore, it can relate the deduced strain to the longitudinal
98 distance in the fiber where it was produced. Additional details of this technology can be found elsewhere
99 in [9,10]. Measurement time lasts from 5 to 20 minutes; therefore, it does not allow to obtain dynamic
100 data. The same system allows to measure from meters to kilometers of distance. In the current setup,
101 about 80m of fibers were used and about 60m were subjected to pile deformation. The error of
102 measurements is of 0.01%. Additional details of the system and examples of measurements can be found
103 in [11,12].
104

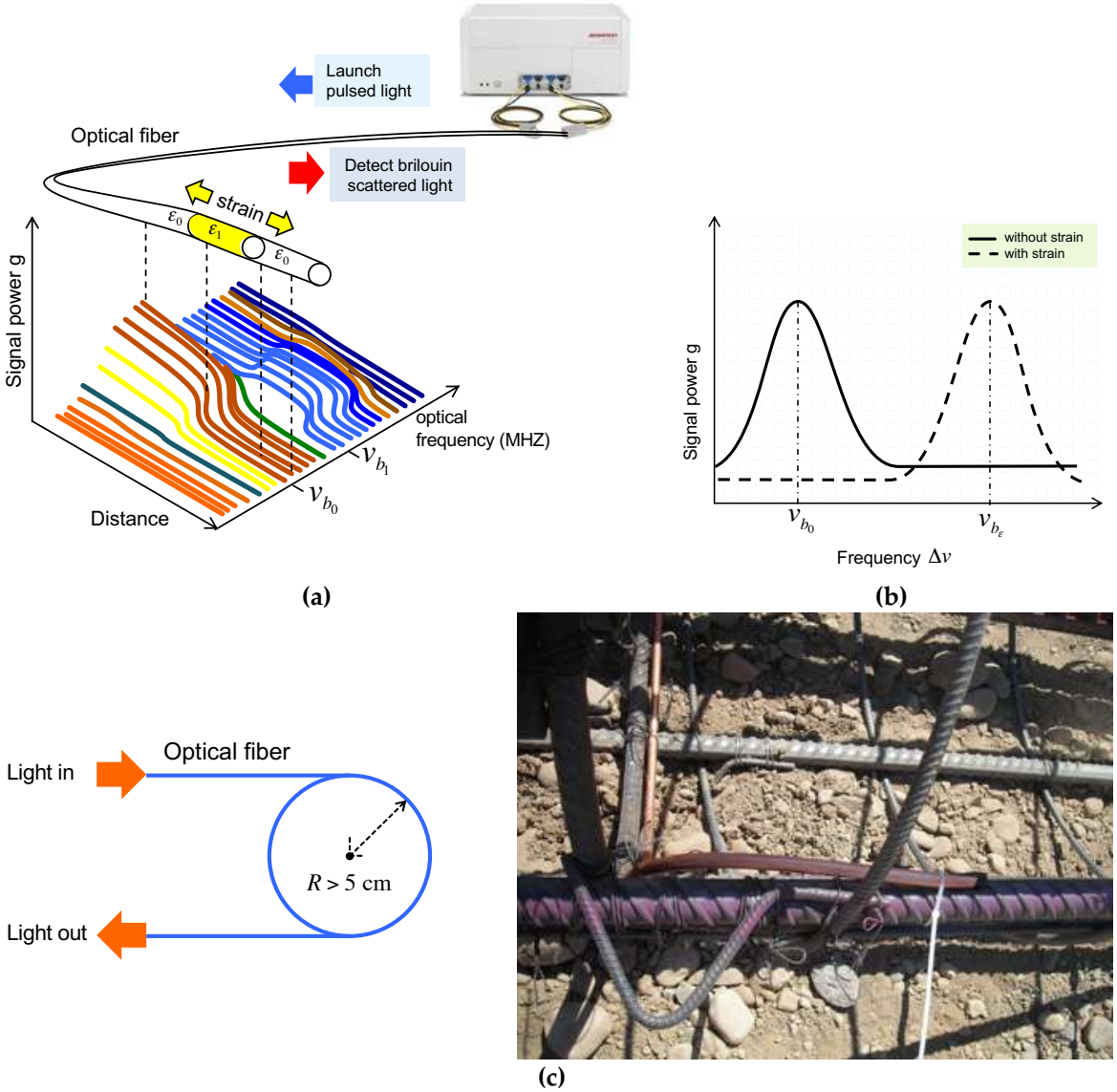

105 **Figure 3.** (**a**) Diagram of a BOTDR equipment; **(b)** change in frequency with strain; **(c)** Minimum curvature
106 for the optical fiber.

The optical fiber was attached to the steel bar using plastic strips, this was a fast and easy task on the field. Bond strength between the optical fiber and concrete is developed as concrete strength increases over time. As light has to travel in the fiber interior then a minimum curvature radio has to be considered with the optical fiber, as shown in Figure 3c. This was done using a copper tube that gives the curvature, protects the fiber and allows the fiber to start the loop to return to the surface (see Figure 3c schema). Figure 4a depicts the location of optical fibers in the pile cross section. Three points are marked with the fiber location, fibers 1 and 2 corresponds to the same fiber (going in opposite directions). Fiber 3 is an independent fiber. The effects of soil excavation in pile strains were obtained by subtracting the base or initial measurement from the fibers to any measurement performed in other specific date.

2.3 Topography survey

The survey equipment used was a station Leica model TC 1800 with an angular precision of 1''. A prism was located in the top part of the pile as shown in Figure 4b. Two fixed points located 20m from the excavation were used as reference.

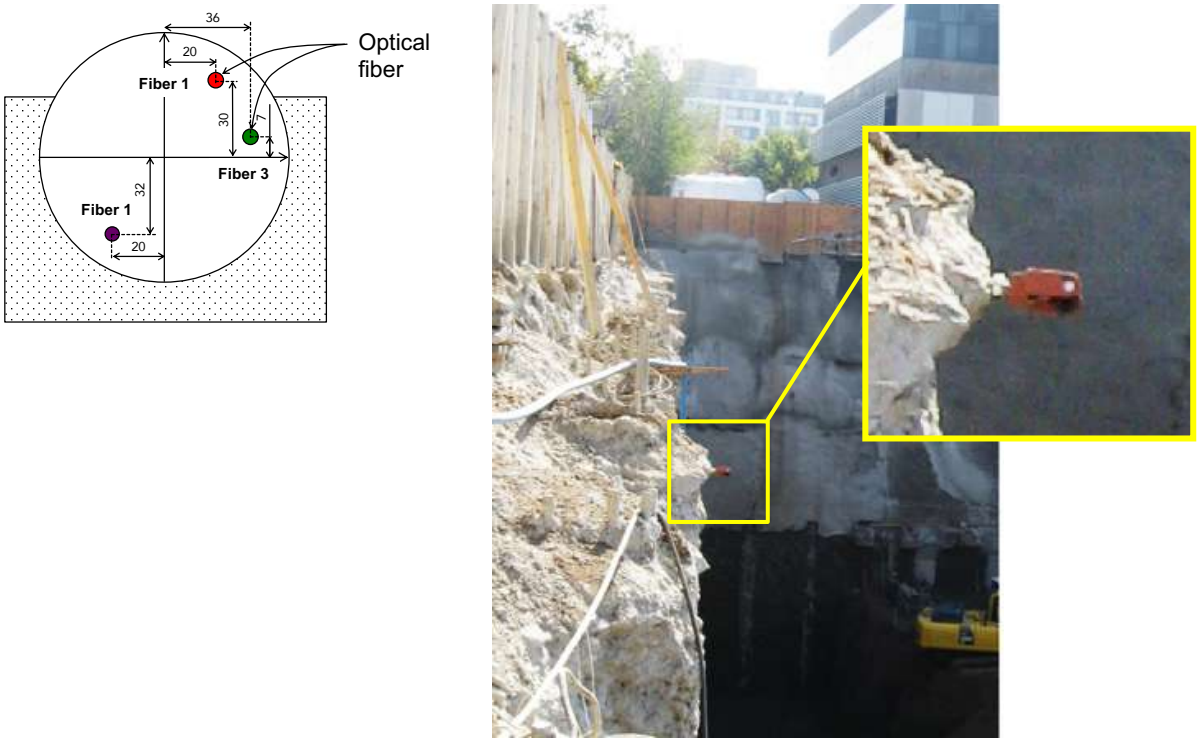

Figure 4. (**a**) Location of optical fibers in the pile; (**b**) Prism used for geodetic measurement.

3. Results

Measurements obtained from strain gauges, optical fiber, inclinometer and survey are presented in this section. Measurements were performed in different construction stages depending on availability due to safety concerns. Figure 5 presents a sketch of the different considered stages and shows the dates when these stages were reached.

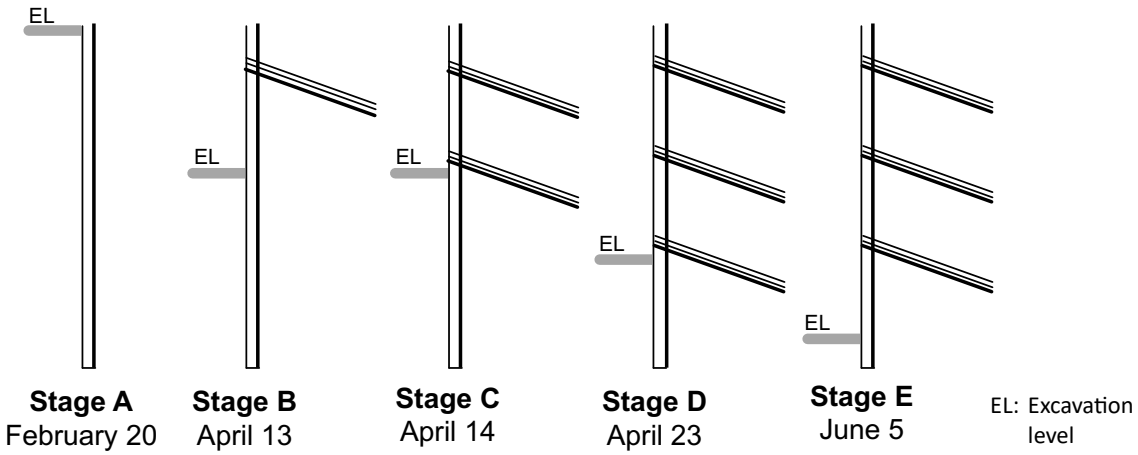

Figure 5. Excavation stages during monitoring using different sensors

3.1 Inclinometer measurements

Inclinometer measurements were performed every 1m approximately. From this data was possible to determine the pile deformation in the direction perpendicular and parallel to the wall. The displacement in the direction parallel to the wall is close to zero. On the other hand, the displacements of the pile in the direction of the excavation are presented in Figure 6.

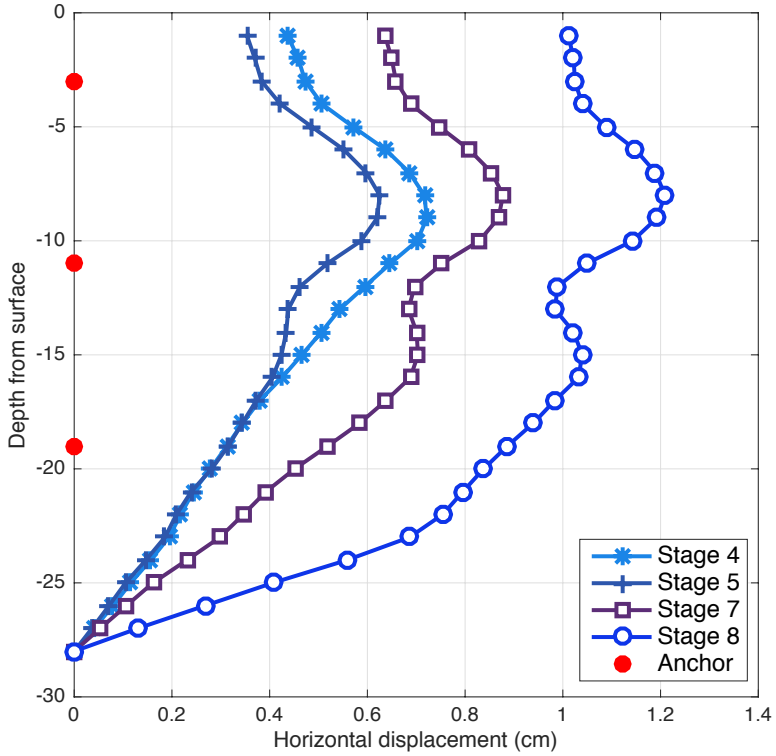

Figure 6. Pile horizontal displacements obtained from inclinometer measurements

The maximum horizontal displacement of the pile is 1.2 cm, as shown in Fig.6. However, these displacements are only the ones corresponding to the integration of the inclinations along the pile. If the pile also experiences rigid body movement, this displacement would not detected by the inclinometer data. In an extreme case the pile could move horizontally a few centimeters without suffering any inclination along its length and therefore the estimated displacements would be zero.

3.2 Optical fiber measurements

As indicated before optical fibers were attached to steel bars in different locations (see Figure 4a). Figure 7a shows an example of measurements using optical fiber (Fiber 1). The initial data (stage A) and the data for stage E along the pile where the optical fiber was attached are shown. Similar measurements were obtained for fibers 2 and 3. The initial data shows that the fiber is under compression, this could occur due to concrete shrinkage during setting/hardening process. To obtain the axial deformation of the pile in each optical fiber, the initial measurements must be subtracted from the measurement of the stage analyzed. In the final stage, two independent measurements are shown for two dates. It is possible to observe that the deformation on the pile-wall does not show changes after 22 days, as expected in gravelly soils.

Figure 7b shows the deduced horizontal displacements perpendicular and parallel to the pile wall. The resulting displacements indicate that the movement parallel to the pile wall is negligible and that the one in the perpendicular direction is close to 1 cm.

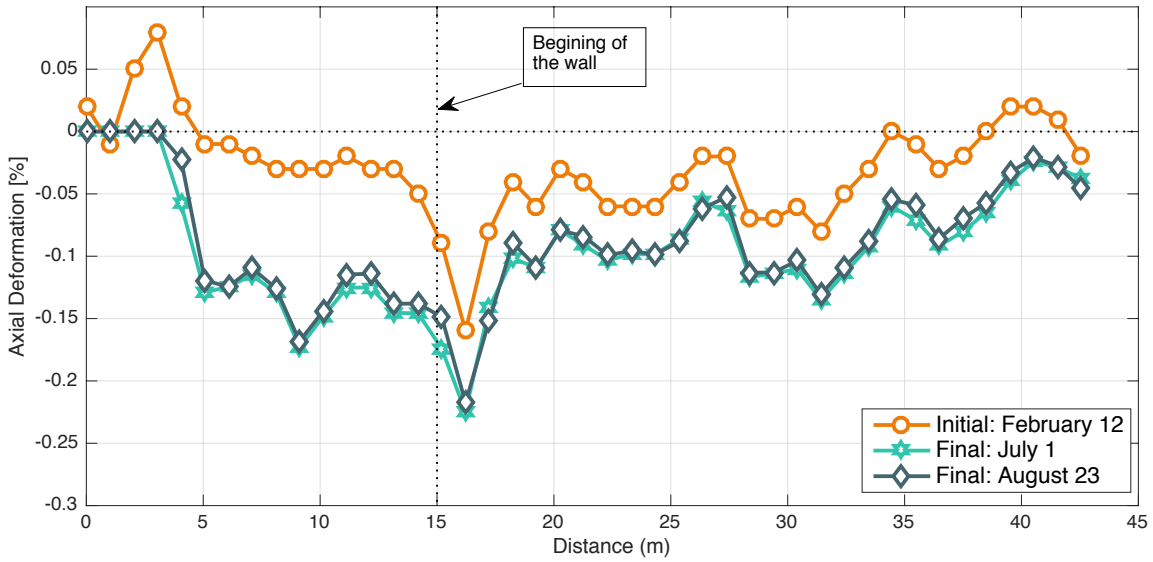

(a)

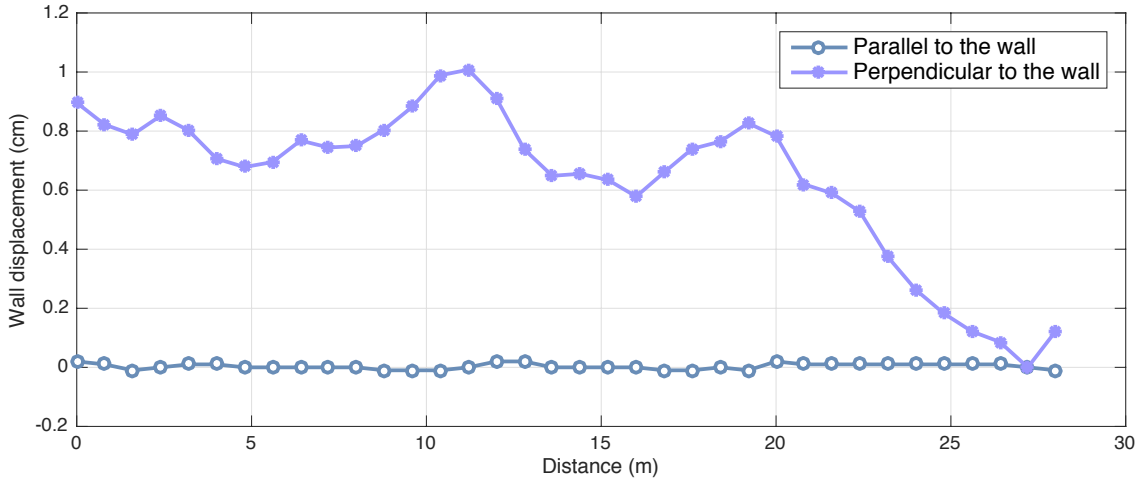

(b)

Figure 7. (a) Initial and stage E measurements on Fiber 1; **(b)** Strain difference between initial and Stage E data

A comparison between estimated displacements from inclinometer measurements and optical fiber is shown in Figure 8a. It can be observed that they are very similar in magnitude, however, the optical fiber sensor seems to capture better the influence of the stressed anchor on pile deformation.

3.3. Strain Gauges measurements

About 50% of the strain gauges were not functioning properly mainly due to the damage they suffered during concrete casting. In this regard, optical fiber and inclinometer showed a better behavior measuring without major inconveniences. Figure 8b shows two lines of strain gauges sensors in comparison with the same location of optical fiber data.

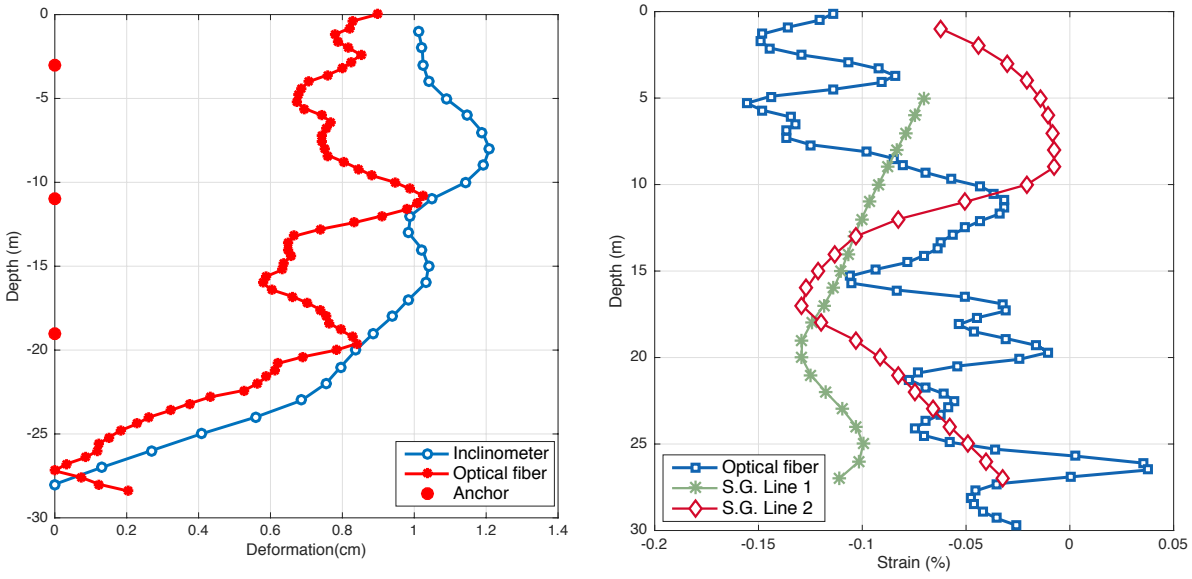

(a) **(b)**

Figure 8. (**a**) Estimated displacements with optical fiber and inclinometers; (**b**) Strain measured by optical fiber and strain gauges

In general, strain gauges showed compression, but the values are not exactly the same. Therefore, due to the distance between strain gauges locations and malfunctioning of about 50% of the sensors this data will not be used to estimate the pile displacements. However, values measured from strain gauges allow us to confirm that measurements obtained from optical fiber and inclinometers are adequate, as are of similar magnitude.

3.4. Topographic survey measurements

Topographic survey performed in stages A and E gives a total lateral displacement of 2.5 cm at the pile top. This value is about 1.5 to 1.6 cm larger than the values estimated from the inclinometer and optical fiber measurements (see Figure 8a). It seems like the difference is caused by a rigid body movement of the pile wall that is not measured by the inclinometer and optical fiber as these methods are not able to capture this type of displacement (see Figure 9a).

Movements measured during this monitoring program consider deformation that occurred during excavation after installation of the anchors. It is also deduced that there was an important component of deformation associated to the base of the excavation. Additionally, deformation can be considered instantaneous as no changes were observed at the same excavation stage after 1 or 2 months. Observed lateral wall movement is plotted together with the relation proposed by Clough et al [6]. as shown in Figure 9b. The maximum lateral movement measured in this research is also included as a straight line in the bottom of this figure.

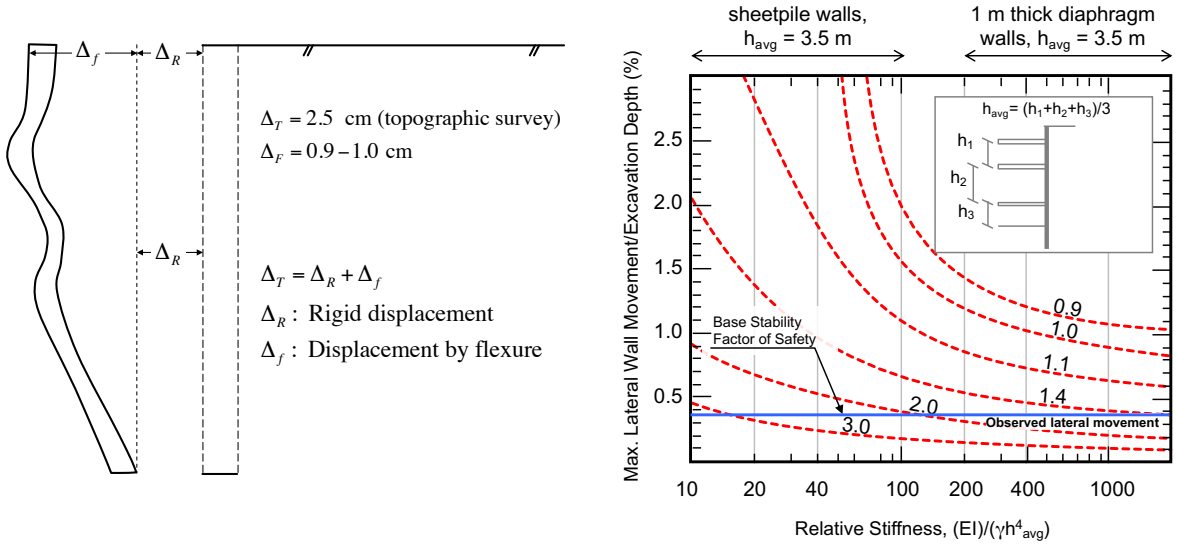

(a) **(b)**

Figure 9. (**a**) Horizontal displacement measured in Stage E; (**b**) Comparison between measured displacements and relationship proposed by Clough et al. [6]

3.5. Numerical modeling

Numerical simulations have been used in the past to reproduce the field measured displacements [13]. Bao et al. [14] evaluated soil-structure systems considering models that include nonlinear material and geometry of both soils and structures. In this research, numerical studies were carried out using the software OpenSees [15] as analysis platform. The wall pile model used nonlinear elements with fibers and force-based formulation. The kinematic relation between strains and displacements was also nonlinear and approximated through a P-delta formulation. The model considered nonlinear uniaxial

197 constitutive relations for concrete and reinforcing bars fibers. The Giuffré-Menegotto-Pinto [16,17] steel
198 material object with isotropic strain hardening was used to model reinforcing bars.
199 This model is capable of representing the hysteretic behavior of steel reinforcement exhibiting the
200 Bauschinger effect together with isotropic strain hardening. Expected yielding stress (480 MPa) was used
201 instead of the nominal value (420 MPa) for nonlinear analysis. Concrete considered a uniaxial model [18–
202 21] with degraded linear unloading/reloading stiffness according to the work of Karsan and Jirsa [22]
203 and no tensile strength. Concrete material was considered unconfined. The peak of the concrete
204 constitutive relation was reduced to account for differences between in place concrete strength and
205 standard cylinder compressive strength f'_c (25 MPa for this case). For large-scale columns common in
206 building construction, a factor C=0.85 is recommended by Moehle [23]. This value, widely adopted in
207 current building codes, was considered for this analysis. Truss elements with an initial stress material
208 were used to model the post-tensioned steel cables. Initial tension force in cables was 600 kN. Slip in the
209 cables active zone was accounted through uniaxial elastic springs of stiffness 6 kN/mm (bottom and
210 middle cables) and 1.5 kN/mm (top cable). Soil-pile interaction was modeled with gap elements (linear
211 elastic behavior in compression and no tension strength). The soil ballast coefficient, used to calculate the
212 gap stiffness in compression, ranged from 6.2 kg/cm^3 to 25 kg/cm^3 close to the pile base. The relevance of
213 the different factors that define the design of these pile walls in practice has also been evaluated.
214 Figure 10a depicts the loads used to represent the earth pressure, obtained from [3]. The value p is
215 obtained as:

$$p = 0.65 K_A \gamma h \quad (2)$$

216 where K_A is the active earth pressure coefficient, γ is the soil unit weight and h the depth below the
217 ground level. Considering typical measured parameters in Santiago gravel, p = 76.05 kN/m. A parametric
218 study was performed to determine the influence of the p value in the expected displacements of the pile-
219 wall.
220 Figure 10b shows the structural response of a 100cm diameter pile for p=76.05 kN/m. A sensitivity
221 study to evaluate the dependence of the estimated displacements on the value of the parameter p was
222 conducted. The range of considered values for p was 70%-130% of the specified value (76.05 kN/m). It is
223 observed that estimated displacements were very sensitive to variations of the specified earth pressure
224 and therefore it is fundamental to have a good estimation of these pressures in practice.
225 From the measured displacement on the field and the numerical model it is possible to deduce that
226 design using expected earth pressure (100%) gives a pile-wall response very similar to the actual
227 observed value on the field using different types of sensors.

228

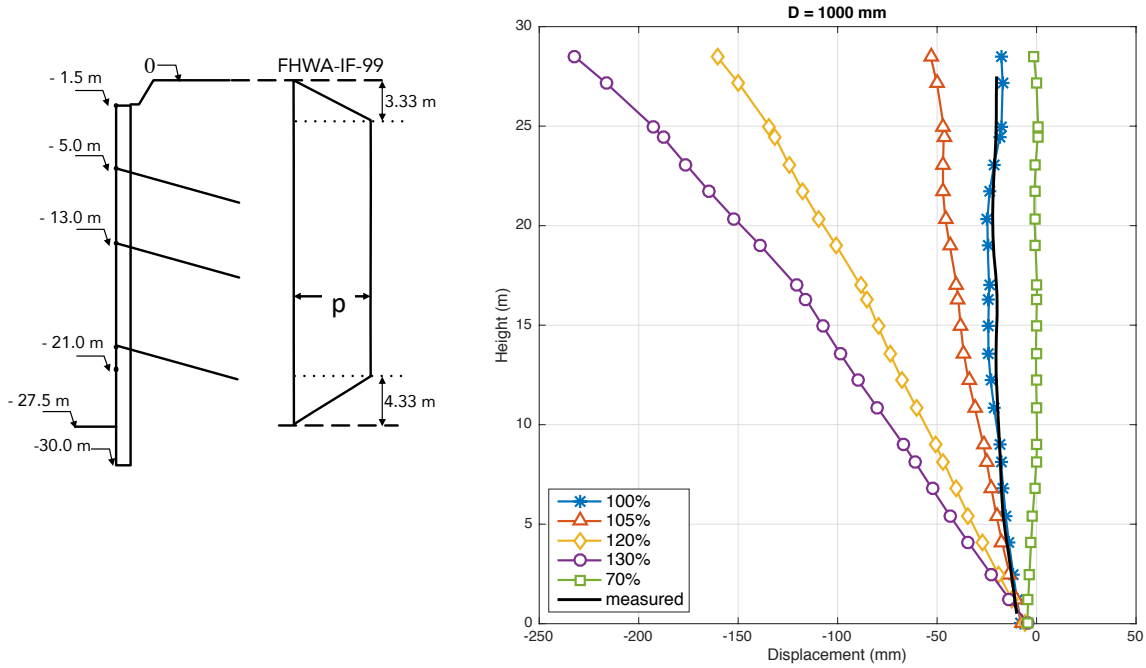

Figure 10. (**a**) Apparent earth pressure for granular material. (**b**) Horizontal displacement (dashed line: measured on site, continuous line: OpenSees model) over the height for different percentages of the specified value p in a 1000 mm diameter pile: 70%, 100%, 105%, 120%, 130%

4. Discussion

Different types of sensors have been used to measured strains and displacement of large pile retaining wall on gravel. These sensors were installed during the construction of a real projects keeping in mind the available time during standard construction of this type of walls. Despite of careful installation of all types of sensors (strain gauges, optical fiber, inclinometer pipes, and survey prism), strain gauges showed to be the most difficult to installed successfully with a relative high number of sensors that do not deliver any data. BOTDR optical fiber shows to be very robust, installation during construction is faster that other methods and despite of concrete been pour inside long piles, there is no major damage on the optical fibers and measurements respond successfully. The use of BOTDR optical fibers appears to be a good option to evaluate performance of deep excavations. Careful interpretation of the data should consider that the movement of deep excavation have a rigid component that is not necessary considered when measuring internal strains of piles/walls, an external measurement must be considered when analyzing the complete movement of this retaining systems.

BOTDR technology should be considered in additional monitoring project involving soil and rock mechanics. It has shown to be easy to install and adequate accuracy, even in actual construction projects.

Numerical modeling and design guidelines agree with the measured displacements. Adequate measurements of strains and displacement allow to check how suitable are current design methods in civil and geotechnical engineering. Field data enable to improve design methods and therefore is necessary to monitor actual projects and publish this data.

5. Conclusions

This paper presents a monitoring program of lateral movement and internal deformation on a 28.5m pile wall on gravelly soil. A companion numerical model was developed to study relevant issues on this retaining wall. Main findings are:

- Displacements of the pile wall were observed exclusively in the direction of the excavation. The horizontal displacement measured at the pile top was 2.5 cm.
- Inclinometers and optical fiber proved to be adequate to measure the deformation of the pile wall. Installation of both systems is simple, and measurements are very stable.
- Deformation in the gravelly soil was instantaneous as expected. After one week, increments in measured displacements were almost negligible.
- Strain gauge installation was slow and close to 50% of them did not work properly after installation. Even though the rest of the strain gauges showed similar strains in comparison to the optical fiber, they did not provide reliable data as other instruments used on site.
- Horizontal displacements estimated from numerical modeling are very sensitive to the magnitude of earth pressure. Therefore, a good estimation is necessary to evaluate wall displacements.
- Displacements of the pile-wall have a rigid displacement movement and a flexural displacement movement. To capture the complete movement is necessary to measure with an external sensor as it was in this case using topographic survey.

Author Contributions: R.M., performed installation and measurements on the field, P.P., performed the numerical models, M.C, analyzed the data, R.M., M.C. wrote, edited the manuscript.

Funding: This research was funded by the Faculty of Engineering, Universidad de Chile.

Conflicts of Interest: The authors declare no conflict of interest.

Appendix A

Table A1. Main characteristics of inclinometer casing.

Type	QC Casing 70 mm (Slope indicator)
Internal diameter	70 mm
External diameter	59 mm
Thickness	11 mm
Maximum pressure	16.5 bar
Maximum load	635 kg
Temperature range	-29 to 88°C

Table A2. Main characteristics of inclinometer.

Probe length	710 mm
Probe diameter	25.4 mm
Probe weight	1.4 kg
Memory	> 1000000 readings
Displacement error	2 mm per 25m
Temperature rating	-40 to 70°C
Data Resolution	0.005 mm per 500 mm

References

1. Moayedi, H.; Tien Bui, D.; Kok Foong, L. Slope Stability Monitoring Using Novel Remote Sensing Based Fuzzy Logic. *Sensors* **2019**, *19*, 4636.

2. Goh, K.H.; Mair, R.J. Response of framed buildings to excavation-induced movements. *Soils Found.* **2014**, *54*, 250–268.
3. Zia, P.; Ahmad, S.; Leming, M. *High-Performance Concretes, A State-Of-Art Report (1989-1994). FHWA-RD-97-030*; Federal Highway Administration, 1997;
4. Hou, Y.M.; Wang, J.H.; Zhang, L.L. Finite-element modeling of a complex deep excavation in Shanghai. *Acta Geotech.* **2009**, *4*, 7–16.
5. Lam, S.Y.; Haigh, S.K.; Bolton, M.D. Understanding ground deformation mechanisms for multi-propped excavation in soft clay. *Soils Found.* **2014**, *54*, 296–312.
6. Clough, G.W.; Smith, E.M.; Sweeney, B.P. *Movement Control of Excavation Support Systems by Iterative Design*; Geotechnical Special Publication.; ASCE: 1989; Vol. 2;.
7. De la Hoz, K. Estimación de los parámetros de resistencia al corte en suelos granulares gruesos. (in Spanish). Master of Science in Engineering, University of Chile: Chile, 2007.
8. Ortigosa, P.; Musante, H.; Kort, I. Propiedades mecánicas de la grava de Santiago.; Santiago, Chile, 1982; pp. 442–454.
9. Thevenaz, L.; Nikles, M.; Fellay, A.; Facchini, M.; Robert, P.A. Truly distributed strain and temperature sensing using embedded optical fibers.; Claus, R.O., Spillman, Jr., W.B., Eds.; San Diego, CA, 1998; pp. 301–314.
10. Mohamad, H.; Soga, K.; Bennett, P.J.; Mair, R.J.; Lim, C.S. Monitoring Twin Tunnel Interaction Using Distributed Optical Fiber Strain Measurements. *J. Geotech. Geoenvironmental Eng.* **2012**, *138*, 957–967.
11. Moffat, R.; Sotomayor, J.; Beltrán, J.F. Estimating tunnel wall displacements using a simple sensor based on a Brillouin optical time domain reflectometer apparatus. *Int. J. Rock Mech. Min. Sci.* **2015**, *75*, 233–243.
12. Moffat, Ricardo A.; Beltran, Juan F.; Herrera, Ricardo Applications of BOTDR fiber optics to the monitoring of underground structures. *Geomech. Eng.* **2015**, *9*, 397–414.
13. Likitlersuang, S.; Surarak, C.; Wanatowski, D.; Oh, E.; Balasubramaniam, A. Finite element analysis of a deep excavation: A case study from the Bangkok MRT. *Soils Found.* **2013**, *53*, 756–773.
14. Bao, Y.; Ye, G.; Ye, B.; Zhang, F. Seismic evaluation of soil–foundation–superstructure system considering geometry and material nonlinearities of both soils and structures. *Soils Found.* **2012**, *52*, 257–278.
15. Mazzoni, S.; McKenna, F.; Scott, M.H.; Fenves, G. *Open system for earthquake engineering simulation: User command-language manual, Pacific Earthquake. OpenSees version 2.0*; Engineering Research Center, University of California Berkeley, 2007;
16. Menegotto, M.; Pinto, P.E. *Method of analysis for cyclically loaded RC frames including changes in geometry and non-elastic behavior of elements under combined normal Force and bending*; IABSE Congress Reports of the Working Commission, 1973;
17. Filippou, F.C.; Popov, E.P.; Bertero, V.V. *Effects of bond deterioration on hysteretic behavior of reinforced concrete joints*; Earthquake Engineering Research Center; University of California, Berkeley, 1983; p. 212;.
18. Kent, D.C.; Park, R. Inelastic behavior of reinforced concrete members with cyclic loading. *Bull. N. Z. Soc. Earthq. Eng.* **1971**, *4*, 108–125.
19. Scott, B.D.; Park, R.; Priestley, M.J.N. *Stress-strain relationships for confined concrete: rectangular sections*; Dept. of Civil Engineering, University of Canterbury, 1980; p. 106;.
20. Hognestard, E. *A study of combined bending and axial load in reinforced concrete members*; University of Illinois Engineering Experimental Station, 1951; p. 129;.

21. Roy, H.E.H.; Sozen, M.A. Proceedings of the International Symposium on Flexural Mechanics of Reinforced Concrete. In Proceedings of the Proceedings of the International Symposium on Flexural Mechanics of Reinforced Concrete; ASCE-ACI, Miami, Fla, 1964.
22. Karsan, I.D.; Jirsa, J.O. Behavior of concrete under compressive loadings. *J. Struct. Div.* **1969**, *95*, 2543–2564.
23. Moehle, J.P. *Seismic design of reinforced concrete buildings*; McGraw-Hill Education: New York, 2015; ISBN 978-0-07-183944-0.